



HAL
open science

Growth Behavior and Electronic Structure of Noble Metal-Doped Germanium Clusters

S. Mahtout, C. Siouani, Franck Rabilloud

► **To cite this version:**

S. Mahtout, C. Siouani, Franck Rabilloud. Growth Behavior and Electronic Structure of Noble Metal-Doped Germanium Clusters. *Journal of Physical Chemistry A*, 2018, 122, pp.662-677. 10.1021/acs.jpca.7b09887 . hal-02290276

HAL Id: hal-02290276

<https://univ-lyon1.hal.science/hal-02290276>

Submitted on 16 Jan 2020

HAL is a multi-disciplinary open access archive for the deposit and dissemination of scientific research documents, whether they are published or not. The documents may come from teaching and research institutions in France or abroad, or from public or private research centers.

L'archive ouverte pluridisciplinaire **HAL**, est destinée au dépôt et à la diffusion de documents scientifiques de niveau recherche, publiés ou non, émanant des établissements d'enseignement et de recherche français ou étrangers, des laboratoires publics ou privés.

Growth Behavior and Electronic Structure of Noble Metal-Doped Germanium Clusters

Sofiane MAHTOUT^{a*}, Chaouki SIOUANI^a and Franck RABILLOUD^{b*}

^a*Laboratoire de Physique Théorique, Faculté des Sciences Exactes, Université de Bejaia, 06000 Bejaia, Algérie*

^b*Univ Lyon, Université Claude Bernard Lyon 1, CNRS, Institut Lumière Matière, F-69622, Villeurbanne, France*

Corresponding authors: mahtout_sofiane@yahoo.fr, franck.rabilloud@univ-lyon1.fr

Abstract:

Structures, energetics and electronic properties of noble metal-doped germanium (MGe_n with $M = Cu, Ag, Au$; $n=1-19$) clusters are systematically investigated by using the density-functional theory (DFT) approach. The endohedral structures in which the metal atom is encapsulated inside a germanium cage appear at $n = 10$ when the dopant is Cu, and $n = 12$ for $M = Ag$ and Au. While Cu doping enhances the stability of the corresponding germanium frame, the binding energies of $AgGe_n$ and $AuGe_n$ are always lower than those of pure germanium clusters. Our results highlight the great stability of the $CuGe_{10}$ cluster in a D_{4d} structure, and to a lesser extent that of $AgGe_{15}$ and $AuGe_{15}$ which exhibits a hollow cage-like geometry. The sphere-type geometries obtained for $n = 10-15$ present a peculiar electronic structure in which the valence electrons of the noble metal and Ge atoms are delocalized and exhibit a shell structure associated with the quasi-spherical geometry. It is found that the coinage metal is able to give both s- and d-type electrons to be reorganized together with the valence electrons of Ge atoms through a pooling of electrons. The cluster size dependence of the stability, the frontier orbital energy gap, the vertical ionization potentials, and electron affinities are given.

1. Introduction

Germanium is an important element in the field of semiconductor materials and the microelectronic industry. Pure and metal-doped germanium clusters have been intensively studied during the last decades in both theoretical and experimental fields, as this class of materials which exhibits size and shape dependent properties provides a rich source to discover new nanostructures with new physical and chemical properties. Their structure and specific properties have been the object of intense researches in order to better understand the stability and growth patterns and to explore the possibility of applications in nanotechnology. Doping Ge_n clusters with a metal atom is expected to significantly change the chemical and physical properties and modify the framework. For example, the dopant atom may stabilize germanium cage structures and induced a large electronic gap.

A large number of investigations on a transition metal encapsulating Ge_n clusters have been carried out¹⁻³³. Zhao and Wang¹ have systematically investigated geometries, stabilities, and electronic properties of $FeGe_n$ ($n = 9-16$) clusters. They found that the doping with one Fe atom contributes to enhance the stability of the germanium clusters and the electron charges always transfer from Fe atom to the neighboring Ge atoms. In the case of $MnGe_n$ ($n = 2-16$) clusters, the same authors² shown that the dopant Mn atom contributes to increase the stabilities of the germanium clusters while the magnetic moment that mainly originates from the unpaired electrons of the 3d state was not quenched when Mn is embedded in Ge_n clusters. Lu and Nagase³ have showed that MGe_{12} ($M = W, Os, Zn$) exhibits a higher chemical stability among MGe_n with $M = Hf, W, Os, Ni, and Zn$, while Ni doped Ge_n clusters have higher

stability as compared to Mn and Co doped Ge_n clusters⁴. For Chromium doped germanium clusters, there are conflicting results. A study has concluded that the Cr atom tends to be located at exohedral positions and do not show tendency to fall into the center of Ge outer frame⁵, while a more recent investigation suggested that CrGe_{10} and CrGe_{14} might be endohedral structures resulting in a quenching of the Cr magnetic moment⁶. However large magnetic moments are found in small $\text{CrGe}_n^{0,+}$ ($n = 1-5$) clusters⁷. Deng et al.⁸ have investigated the structural, electronic and magnetic properties of $\text{VGe}_n^{-/0}$ ($n = 3-12$) clusters. They found an electron transfer from Ge atoms to the V atom and related the minimization of the magnetic moments to the structural pattern. In the case of TM@Ge_n ($\text{TM} = \text{Ti, Zr and Hf}$; $n = 1-20$) clusters, Kumar et al.⁹ found that the clusters having 20 valence electrons turn out to be relatively more stable in both the neutral and the anionic series. Also, the TM atom is adsorbed endohedrally in the pure germanium cage for $n > 9$ and the spin on the TM atom is quenched for clusters with $n > 7$. Similarly, Bandyopadhyay and Sen¹⁰ have showed that NiGe_n clusters having 20 valence electrons are relatively more stable in both neutral and cationic species. Wang and Han¹¹⁻¹⁴ investigated CuGe_n ($n=2-13$), NiGe_n ($n=1-13$), WGe_n ($n=1-17$) and Mo_2Ge_n ($n= 9-15$) clusters. They show that the doping with Cu atom decreases the binding energies while the doping with Ni or W strengthens the stability of germanium clusters. Studying the properties of neutral and cationic MoGe_n ($n=1-20$) clusters, Trivedi et al.¹⁵ have showed that clusters containing more than nine germanium atoms are able to absorb a Mo atom endohedrally into a germanium cage and the spin magnetic moment of the Mo atom is quenched in all Mo-doped Ge_n clusters. The most stable structures of Mo_2Ge_n ($n= 9-13$) clusters have one Mo atom inside a Ge_n cage and another Mo atom on the surface at smaller cluster sizes while the Mo_2 dimer is completely encapsulated into the germanium clusters when the cluster size increases to 15¹⁴. For CoGe_n clusters, the magnetic moment is not quenched, the doping of the Co atom generally enhances the stability of the host Ge_n clusters and the Co atom is completely falls into the center of the Ge outer frame from $n= 9$ ¹⁶⁻¹⁷. Singh et al.¹⁸ have reported from *ab initio* calculations that thorium encapsulation can be used to stabilize highly symmetric cages of germanium with 16 and 20 atoms. $\text{Bi}_2\text{Ge}_{n-2}$ ($n= 3-8, 12$) clusters¹⁹ have been found to be characterized by high stability and symmetry and relatively large highest occupied-lowest unoccupied molecular orbital energy gaps (HOMO-LUMO gaps). ZrGe_n clusters²⁰ have been predicted to stabilize cage-like structures for $n \geq 13$. Structural and electronic properties of Ruthenium doped germanium clusters have been performed using a particle swarm optimization metaheuristic coupled with density functional theory computations by Jin et al²¹. They found that there is an inherent tendency of the formation of an endohedral cage of RuGe_n clusters with increasing stability as the size increase. More recently, we found that the vanadium atom in VGe_n can largely contribute to strengthen the stability of the framework from $n = 7$, while the cage-like VGe_{14} cluster with a high symmetry and a high stability exhibits a peculiar electronic structure in which the valence electrons of V and Ge atoms are delocalized and exhibit a shell structure associated with the quasi-spherical geometry. This cluster is proposed to be a good candidate to be used as the building blocks for developing new materials²². In experiment, the anion photoelectron spectroscopy has been performed for some germanium clusters containing transition or lanthanide-metal atom²³.

Although the doping of Ge_n with a transition metal atom have been intensively studied, there is no systematic investigation on the doping by a noble metal atom in literature to the best of our knowledge. However some recent studies have considered small clusters in a limited size range. Li et al.²⁴ have studied the size-selective effects of geometrical structures and electronic properties on neutral and anionic $\text{AuGe}_n^{0/-}$ ($n = 1-13$) clusters. Their results indicate that the addition of an extra electron to neutral cluster may enhance its kinetic

stability. Recently, the photoelectron spectroscopy of small AuGe_n^- clusters revealed an electronic structure and a very high detachment energy for AuGe_{12}^- compatible with a high-symmetry geometry like I_h structure²⁵. Bandyopadhyay²⁶ has reported endohedral structures for CuGe_n clusters with $n > 7$, while the doping of Ge_9 and Ge_{10} with several types of metal atoms including noble metals have been also considered²⁷⁻²⁹. Interestingly, the global minimum of CuGe_{10}^+ clusters were presented to be a magic cluster with D_{4d} symmetry and 40 valence electrons that satisfy the jellium electron shell model³⁰. The authors also proposed a concept of doubly spherical aromatic based on a counting rule for both pi-type and sigma-type valence electrons²⁸.

Here we present a systematic investigation of the geometry, relative stabilities, and electronic properties of coinage metal germanium doped clusters MGe_n ($\text{M}=\text{Cu, Ag, Au}$; $n = 1 - 19$) in the framework of the density-functional theory (DFT). We aim to highlight the modifications in the properties of Ge_n clusters due to the doping atom, and to study the role of the nature of the dopant coinage metal atom. It is hoped that this work would be useful to understand the influence of different noble metal on the properties of germanium clusters and could provide powerful guidelines for future experimental studies. The present paper is organized as follows: In Section 2, we describe our theoretical approach. The structural and energetic properties of MGe_n clusters ($n = 1-19$) clusters are presented sections 3, following by a discussion about the electronic properties.

2. Computational methodology

Spin polarized calculations are carried out by generalized gradient approximation (GGA) with PBE exchange-correlation functional³⁴. Self-consistent field procedures are carried out with a convergence criterion of 10^{-4} a.u. on the energy and electron density. Calculations have been performed by using the method of norm-conserving Troullier-Martins nonlocal pseudo-potentials³⁵ in the Kleinman-Bylander projectors³⁶ as implemented in SIESTA packages³⁷. We used a double zeta basis plus polarization orbitals (DZP) for dopant atoms species (Cu, Ag, Au) and double zeta basis (DZ) for Ge atoms. In order to avoid interaction between neighboring clusters, a large cubic cell of 40 Å edge lengths with a periodic boundary condition is taken. The k grid integration has been carried using the Γ point approximation. The atomic positions have been optimized by the conjugate gradients dynamics algorithm until the residual forces are smaller than 10^{-3} eV/Å, and without any symmetry constraints. Further analysis of the electronic properties and molecular orbitals have been performed with the software Gaussian09³⁸ using PBE and the Gaussian-type basis sets cc-pvtz for Ge and LanL2DZ for coinage metal atoms.

The number of geometric isomers or local minima increases exponentially with the cluster size. For this reason, lots of putative isomers including some high and low symmetries were relaxed for each cluster size. Amongst them, some initial structures of Ge_{n+1} and metal-doped Ge_n clusters were taken from literature^{5,10-11,22,39-40}. Also, the putative structures of MGe_n were obtained by local relaxation after the substitution of one Ge atom by M atom in several isomers of the original pure Ge_{n+1} cluster. The different initial positions of the Ge atom in the Ge_{n+1} clusters lead to different MGe_n isomers. But the search for the lowest isomer cannot include a global optimization procedure of the potential energy surface, and we cannot be sure that a more stable structure than those found in our calculations does not exist. In the next section, we only show the best calculated structures for each cluster size. The spin state of all clusters is found to be singlet or doublet for even and odd number of electrons respectively.

In order to check the reliability of our computational method, the dimers Ge₂, Cu₂, Au₂ and Ag₂ dimers were first considered. The bond lengths of Ge₂, Ag₂, Au₂ and Cu₂ were calculated to be 2.450, 2.595, 2.627, and 2.280 Å respectively. These values are in good agreement with the experimental data of 2.57 (Ref [41]) and 2.44 Å (Ref [42]) for Ge₂, 2.53 Å for Ag₂ (Ref [43]), 2.47 Å for Au₂ (Ref [44]), and 2.22 Å for Cu₂ (Ref [45]). The binding energy per atom, calculated to be 1.44, 1.07, 1.37 and 1.13 eV for Ge₂, Ag₂, Au₂ and Cu₂ respectively, are also in good agreement with both theoretical and experimental data^{11,26,46-47}.

3. Results

3a Structural properties

The lowest energy been structures of pure Ge_n clusters have already reported in the literature²². Shortly, the lowest-energy isomer of the trimer Ge₃ presents a *D*_{3h} triangular geometry, while that of Ge₄ is a rhombus structure with *D*_{2h} symmetry. The triangular bipyramid framework with *D*_{3h} symmetry is found to be the global minimum structure of the Ge₅ pentamer. The hexamer Ge₆ has two lowest-energy isomers quasi-degenerate, the first one is a bicapped quadrilateral structure with *C*_{2v} symmetry and the second one shows a bicapped rectangular geometry with *D*_{4h} symmetry. The most stable isomer of the heptamer Ge₇ adopts a structure having *C*₂ point group symmetry. The ground state structure of Ge₈ cluster can be seen as a capped pentagonal bipyramid with *C*_s symmetry. The Ge₉ cluster forms a capped cube like structure with *C*_{4v} symmetry. For Ge₁₀, the most stable structure is a capped irregular pentagonal prism structure with *C*₁ symmetry. Ge₁₁ is a capped pentagonal structure with *C*_{2v} point group symmetry. Ge₁₂ displays a compact and nearly spherical structure with *C*_{2v} symmetry. For the clusters size range between 13 and 16, a prolate geometry with *C*₁ point group symmetry is always favored. The lowest-energy structure of Ge₁₇ presents a nearly spherical shape with *C*_s symmetry while a prolate-like structure with *C*₂ symmetry is observed in the case of Ge₁₈. The ground state isomer for Ge₁₉ has a prolate shape with *C*_{2v} point group symmetry, while the best structure of Ge₂₀ adopts a cage like structure with lower symmetry.

We now discuss optimized geometries for the three systems MGe_n (M = Cu, Ag, Au) in the size range of n = 1 to 19. The lowest energy structures together with some low-lying isomers are presented in Figure 1, 2 and 3 for AgGe_n, AuGe_n and CuGe_n respectively. Meanwhile, the corresponding symmetry group, binding energy per atom, HOMO-LUMO gap, vertical ionization potential, vertical electronic affinity, and average bond lengths *a*_{Ge-Ge} and *a*_{Ge-M} (M=Cu, Ag, Au) are summarized in Table 1, 2 and 3 for AgGe_n, AuGe_n and CuGe_n respectively.

Both AgGe and AuGe dimers have a binding energy per atom of 0.813 eV which is 0.372 eV less stable than the dimer CuGe. The bond lengths are calculated to be 2.591, 2.645 and 2.333 Å for AgGe, AuGe and CuGe respectively. For CuGe, our present data are very near to those predicted by Bandyopadhyay²⁶.

For small clusters, the lowest-energy isomers are similar whatever the nature of the doping atom M = Ag, Au, or Cu. A triangular structure with *C*_{2v} symmetry is found for MGe₂ and a planar rhombus with *C*_{2v} symmetry is found for MGe₃. For CuGe_n (n=1-3) clusters our results are similar to those reported by Bandyopadhyay²⁶. The best isomer of MGe₄ can be

seen as a distorted Ge₄ rhombus with a capped dopant on one face. For MGe₅ clusters, the metal M atom is capping a Ge₅ triangular pyramid. Up to size n = 8, the structures of MGe_n clusters are roughly similar for M = Ag, Au and Cu. The substitution of one germanium atom by one noble metal atom in the capped bi-pyramid pure Ge₈ structure gives the optimized ground state structure of MGe₇ with M atom capping a pentagonal by-pyramid. The structure of MGe₈ can be seen as MGe₆ on which two additional Ge atoms are localized on surface, or alternatively it can also be seen as a distorted cube-like MGe₇ structure with a capping Ge atom.

Starting from n = 9, the optimized structures of Cu-doped Ge_n clusters differ from those of Ag- and Au-doped Ge_n. A prolate-like structure with the M atom located out of the frame of germanium cluster is obtained as the best isomer of MGe₉ clusters. Cu atom is highly coordinated to the neighboring Ge atoms in CuGe₉ comparatively to Ag and Au atoms in AgGe₉ and AuGe₉ clusters. The endohedral structures in which the metal atom is encapsulated inside a germanium cage appear at n= 10 when the dopant is Cu, and n = 12 for M = Ag and Au. Indeed, the lowest-energy structure of CuGe₁₀ is a *D*_{4d} symmetry cage-like structure with Cu atom highly coordinated at the center of the cage. This structure has been already found previously²⁷. CuGe₁₁ has also a cage-like structure with a Cu atom highly coordinated. In contrast, Ag and Au atoms are still in peripheral position in MGe₁₀₋₁₁. All ground states isomers of MGe₁₂ are high symmetry cage-like structures with M atom highly coordinated at the center of the germanium cage. The lowest-energy isomer of CuGe₁₂ belongs to the high-symmetry *D*_{5d} point group while that of AgGe₁₂ and AuGe₁₂ clusters has a *D*_{2d} symmetry. The latter can be described as a biccapped pentagonal prism and were previously proposed by Li et al.⁴⁸ as a putative structure for AuGe₁₂, lying below the hexagonal prism with *C*_s symmetry (isomer *e*) well known to be the ground state for several transition metal Ge doped clusters^{22,49}. The isoelectronic cluster RuGe₁₂³⁻ is also found to lie in the *D*_{2h} structure⁵⁰. Previous works on the anion AuGe₁₂⁻ have furnished conflicting results since Li et al.²⁴ has predicted a *D*_{2d} structure to be the lowest-isomer with hybrid DFT + MP2 level calculations, while Lu et al.²⁵ obtained a *I*_h-symmetry structure using DFT + CCSD calculations. The latter is in better agreement with the photoelectron spectroscopy results²⁵. In our calculation, we find that the *I*_h-symmetry structure is the most stable isomer for the anion while the neutral AuGe₁₂ cluster adopts a *D*₂-symmetry structure. For AgGe₁₂, the *D*_{5d} symmetry structure is found to be stable but lying 0.09 eV above the *D*_{2d} structure.

From n=13 to n = 19, Cu occupies an endohedral position for each size. Ag and Au are generally located in a cage-like structure with some exceptions for AgGe_{15,16,18} and AuGe_{15,18}, where the metal atom prefers a peripheral position with a low number of coordination. Interestingly, the most stable isomer of MGe₁₄ is a cage belonging a high symmetry *D*_{4h} point group for the three metal M = Ag, Au, Cu. A high *O*_h symmetry have been previously predicted to be highly stable for W- or V-encapsulated Ge₁₄ clusters^{13,22} but for noble metal atom the *O*_h symmetry structure was found to relax in a *D*_{4h} symmetry geometry. As we can see clearly from Tables 1 and 2, the average Ge-Ag and Ge-Au bond lengths are larger than the average Ge-Ge bond length. In contrast, the average Ge-Cu bond length is smaller than the average Ge-Ge bond length as we can see from Table 3. These parameters can significantly affect the stability and others properties of each MGe_n species.

3b Energetics

The binding energy par atom of MGe_n clusters is defined as

$$E_b(MGe_n) = (n E(\text{Ge}) + E(\text{M}) - E(MGe_n)) / (n+1),$$

where $E(\text{Ge})$ is the total energy of free Ge atom, $E(\text{M})$ the total energy of free $\text{M} = \text{Ag}, \text{Au}, \text{Cu}$ atom and $E(MGe_n)$ is the total energy of the MGe_n cluster. The calculated binding energies for all clusters are reported in Table 1, 2 and 3, and their evolution with the cluster size n is shown in Figure 4 for the best isomers of each system. For comparison, the evolution of binding energy of their corresponding ground state pure germanium clusters is also plotted. As expected, the binding energy generally increases with increasing size, which means that these clusters can continuously gain energy during the growth process. This is likely associated to the increase in the average number of neighbors per atom. The binding energy per atom of all systems increases rapidly from $n=1$ to $n=6$, then a slow and non-monotonic growth is observed. The Cu doping atom enhances the stability of the corresponding Ge_n frame from $n = 10$, i.e. when $CuGe_n$ clusters adopt cage-like structures with Cu atom highly coordinated at central position. In contrast, the binding energies of $AgGe_n$ and $AuGe_n$ are always lower than those of pure germanium clusters, $AgGe_n$ clusters being slightly more stable than gold-doped clusters. This behavior can be due to the nature of the bonding involving Cu, Ag and Au species, since copper presents a stronger covalent character than Ag and Au and a greater ability to make chemical bonds⁵¹. For copper-doped clusters, a pronounced value of binding energy is observed at $n=10$ and 12 in which Cu is encapsulated in a quasi-perfect Ge_n cage. The binding energies per atom for $CuGe_{10}$ and $CuGe_{12}$ are calculated to be 3.080 and 3.099 eV respectively. They are somewhat similar to the binding energy of 3.058-3.179 eV calculated for VGe_{10-15} cage-like structures²². For $AgGe_n$ and $AuGe_n$, the largest value is obtained at $n = 15$, with 3.019 and 2.997 eV/atom respectively, and corresponding to a peculiar hollow cage-like geometry where the metal atom is inserted into the germanium structure without having a particular position.

In cluster physics, the second-order difference in energy (Δ_2E) can well reflect the relative stabilities of the corresponding clusters. It is generally compared with the relative abundances determined in mass spectroscopy experiments. For the ground-state MGe_n clusters, it can be calculated as

$$\Delta_2E = E(MGe_{n+1}) + E(MGe_{n-1}) - 2 E(MGe_n),$$

where E is the total energy of the ground state cluster. In Figure 05, we show the variation of Δ_2E as a function of the size n . The plots show some pronounced positive peaks at $n = 5, 8, 12$ and 15 for all MGe_n ($\text{M}=\text{Cu}, \text{Ag}, \text{Au}$) clusters. A relative high stability is found for $CuGe_{10}$, $CuGe_{12}$, $AgGe_{10}$, $AgGe_{12}$, $AgGe_{15}$, $AuGe_{12}$ and $AuGe_{15}$. It is mainly due to the metal-germanium bonds since the corresponding initial pure germanium clusters do not show a peculiar stability.

The chemical activity of clusters can be characterized by the measurement of the HOMO–LUMO gap. In general, a large HOMO-LUMO gap implies a low chemical activity and a high chemical stability, while the latter decreases as the HOMO-LUMO gap decreases. The calculated HOMO-LUMO gaps for all $AgGe_n$, $AuGe_n$ and $CuGe_n$ clusters are reported in Table 1, 2 and 3 respectively. Their evolution as a function of the size for the ground states structures is plotted in Figure 06. The decreasing tendency with increasing size is strong for pure germanium clusters but less significant for metal-doped Ge_n clusters. As expected, the gap of MGe_n is lower than that of the pure Ge_{n+1} cluster, except for sizes $n= 10$, indicating that the metal dopant in the germanium clusters generally increases the chemical activity of

clusters. Values oscillate in the 0.15-1.3 eV range but the evolution with the cluster size shows a non-monotonic behavior. Pronounced value of HOMO-LUMO gaps are observed at $n = 4, 6, 13, 15$ and 18 for AgGe_n and at $n = 4, 6, 10, 13, 16$ and 18 for AuGe_n and at $n = 5, 10, 13, 16$ for CuGe_n clusters which indicate that these clusters have a higher stability and a low reactivity than their neighbors. Particularly, the high relative value of 1.324 eV for CuGe_{10} reflects the chemical stability of this cluster which may likely be a good candidate to be used as a building block for developing new materials.

The vertical electroaffinity (VEA) and vertical ionization potential (VIP) are defined as $VEA = E(MGe_n) - E(MGe_n^-)$ and $VIP = E(MGe_n^+) - E(MGe_n)$, where $E(MGe_n^-)$ and $E(MGe_n^+)$ are the energy of the corresponding anionic and cationic clusters calculated at the geometry of the neutral system. The obtained calculated VEA and VIP are reported in Tables 1, 2 and 3, while their evolutions as a function of the cluster size are plotted in Figure 07 and Figure 08 together with those of Ge_{n+1} clusters. These data could be compared to experiment even if to our knowledge no experimental data are available nowadays. The VEA values present a non-monotonic increasing with the cluster size, while the VIP values present a non-monotonic decreasing with the cluster size. Both VEA and VIP are relatively few dependent on the nature of the doping metal, even if values for copper-doped clusters are often slightly larger than those for Ag- and Au-doped clusters. CuGe_{12} , with its highly D_{5d} symmetry structure, presents the highest values.

4 Discussion

Our results highlight a great stability for CuGe_{10} cluster in an endohedral structure. This is line with the experimental mass spectrometric stability investigation by Lievens et al.⁵² that exhibited remarkably high abundance for CuGe_{10}^+ and interpreted it in terms of peculiarly stable dopant-encapsulated cage-like structures. In Ref [27], the 42 valence electrons (4 from Ge and 1 for Cu) in CuGe_{10}^- are found to be distributed in the following energy sequence of electronic shell model [$1S^2 1P^6 1D^{10} 1F^2 2S^2 1F^8 2P^2 1F^4 2P^4 1G^2$]. In our work, the d electrons of Cu are found to participate as well to the delocalized orbitals and then 51 electrons (4 from Ge and 11 from Cu) are in the delocalized electronic shells with the following filling [$1S^2 1P^6 1D^{10} 2D^{10} 2S^2 1F^{14} 2P^6 1G^1$]. Due to a lowering symmetry (D_{4d} instead of K_h for a sphere), some shells are splitting subshells. However one can expect that the number of electrons fit with shell closings numbers for the cation CuGe_{10}^+ , and such an organization contributes to the high stability of the cluster through the pooling of electrons. Density of states (DOS) together with representative Kohn-Sham orbitals are given in Figure 9 for $\text{CuGe}_{10,12,14}$. All molecular orbitals can be found in Supporting Information. We can easily distinguish the orbitals associated to S, P, D, F, G supershells. For the endohedral structure corresponding to the lowest-energy isomer of CuGe_n , with $n > 14$, we were not able to assign a symmetry character of molecular orbitals, and we think the supershell filling is no more valid. The great values of VIP and VEA calculated for CuGe_{12} is due to the high symmetry (D_{5d}) of its geometrical structure resulting to a large gap between two successive electronic shells (Figure 9).

We show in figure 10 the density of states (DOS) for the lowest-energy isomer of $\text{AgGe}_{12,14,15}$, and $\text{AuGe}_{12,14,15}$. These structures are of sphere-type where the germanium cage encapsulates the metal atom resulting in a high symmetry structure, except for $n=15$, where the metal atom is inserted into the germanium structure without having a particular position, resulting in a hollow cage-like geometry. Our above results highlight a relative high stability

for $n = 15$. As a matter of fact, the electronic configuration of AgGe_{15} and AuGe_{15} , $[1S^2 1P^6 2S^2 1D^{10} 1F^{14} 3S^2 2D^{10} 2P^6 1G^{18} 1H^1]$ see Table 4, fits well with shell closings numbers with a single excess electron, similarly to the configuration found for CuGe_{10} . The high stability of the three clusters, CuGe_{10} , AgGe_{15} and AuGe_{15} , can be explained by such organization. The Kohn-Sham molecular orbitals of AgGe_{15} and AuGe_{15} are showed in Supporting Information, we can note that the molecular orbitals 1F, 2D, and 1G are mixed. It is very significant that the coinage metal is able to give both s- and d-type electrons to be reorganized together with the valence electrons of Ge atoms through a pooling of electrons. To the best of our knowledge, that has never been reported previously. And it is in line with the recent photoelectron spectroscopy results on small AuGe_n^- which has suggested strong interactions between the 5d orbitals of the Au atom and the 4s4p hybridized orbitals of the Ge atoms²⁵.

The electron shell configuration of endohedral cage-like structure MGe_n ($M = \text{Cu, Ag, Au}$; $n = 10, 12, 14$) and hollow cages of AgGe_{15} and AuGe_{15} are given in Table 4. The density of states together with Kohn-Sham molecular orbitals can be found in Supporting information. The orbitals character can be easily identified for all cages, even if some mixing were found for 2D-, and 1G-type orbitals in case of low-symmetry geometries.

5. Conclusion

We have performed a systematic investigation on the coinage metal-doped germanium (MGe_n with $M = \text{Cu, Ag, Au}$; $n=1-19$) clusters by using first-principles DFT calculations. Doping with Cu atom enhances the stability of the corresponding germanium frame when CuGe_n clusters adopt cage-like structures with Cu atom highly coordinated at central position. In contrast, the binding energies of AgGe_n and AuGe_n are always lower than those of pure germanium clusters. The endohedral structures in which the metal atom is encapsulated inside a germanium cage appear at $n = 10$ when the dopant is Cu, and $n = 12$ for $M = \text{Ag}$ and Au. Our results highlight the great stability of the CuGe_{10} cluster in D_{4d} structure which exhibits a large binding energy, a large frontier orbital energy gap, and a relative small electron affinity. AgGe_{15} and AuGe_{15} which exhibit a hollow cage-like geometry where the metal atom is inserted into the germanium structure without having a particular position present a relative high stability as well. The sphere-type structures obtained for $n = 10-15$ present a peculiar electronic structure in which the valence electrons of the noble metal and Ge atoms are delocalized and exhibit a shell structure associated with the quasi-spherical geometry. Each Ge gives 4 electrons while each coinage atom gives 11 electrons. It is very significant that the coinage metal is able to give both s- and d-type electrons to be reorganized together with the valence electrons of Ge atoms through a pooling of electrons. We hope that the present study will motivate appropriate experimental investigations probing the electronic properties and the stability of noble metal-doped germanium clusters.

Acknowledgement

FR thanks the Pôle Scientifique de Modélisation Numérique (PSMN) at Lyon, France, and the GENCI-IDRIS (Grant i2016086864) center for generous allocation of computational time.

Supporting Information. Density of states for the most stable and low-lying isomers of $\text{CuGe}_{10,12,14}$, $\text{AgGe}_{12,14,15}$, and $\text{AuGe}_{12,14,15}$, together with Kohn-Sham molecular orbitals.

References

- [1] Zhao, W. J.; Wang, Y. X. Geometries, stabilities, and electronic properties of FeGe_n (n = 9–16) clusters: Density-functional theory investigations. *Chem. Phys.* **2008**, *352*, 291–296.
- [2] Zhao, W. J.; Wang, Y. X. Geometries, stabilities, and magnetic properties of MnGe_n (n = 2–16) clusters: Density-functional theory investigations. *J. Mol. Str.: THEOCHEM* **2009**, *901*, 18–23.
- [3] Lu, J.; Nagase, S. Metal-doped germanium clusters MGe_n at the sizes of n = 12 and 10: Divergence of growth patterns from the MSi_n clusters. *Chem. Phys. Lett.* **2003**, *372*, 394–398.
- [4] Kapila, N.; Jindal, V. K.; Sharma, H. Structural, electronic and magnetic properties of Mn,Co, Ni in Ge_n for (n=1-13). *Physica B* **2011**, *406*, 4612-4619.
- [5] Kapila, N.; Garg, I.; Jindal, V. K.; Sharma, H. First principle investigation into structural growth and magnetic properties in Ge_nCr clusters for n=1-13. *J. Magnetism and Magnetic Mat.* **2012** *324*, 2885-2893.
- [6] Dhaka, K.; Bandyopadhyay, D. Study of the electronic structure, stability and magnetic quenching of CrGe_n (n=1-17) clusters: a density functional investigation. *RSC ADVANCES* **2015**, *5*, 83004-83012.
- [7] Hou, X.-J.; Gopakumar, G.; Lievens, P.; Nguyen, M. T. Chromium-doped germanium clusters CrGe_n (n = 1-5): geometry, electronic structure, and topology of chemical bonding. *J. Phys. Chem. A* **2007**, *111*, 13544-13553.
- [8] Deng, X.-J.; Kong, X.-Y.; Xu, H.-G.; Xu, X.-L.; Feng, G.; Zheng, W.-J. Photoelectron spectroscopy and density functional calculations of VGe_n⁻ (n = 3-12) Clusters. *J. Phys. Chem. C* **2015**, *119*, 11048–11055.
- [9] Kumar, M.; Bhattacharyya, N.; Bandyopadhyay, D. Architecture, electronic structure and stability of TM@Ge_n (TM = Ti, Zr and Hf; n = 1-20) clusters: a density functional modeling. *J. Mol. Model.* **2012**, *18*, 405-418.
- [10] Bandyopadhyay, D.; Sen, P. Density functional investigation of structure and stability of Ge_n and Ge_nNi (n = 1-20) clusters: validity of the electron counting rule. *J. Phys. Chem. A* **2010**, *114*, 1835-1842.
- [11] Wang, J.; Han, J.-G. A computational investigation of copper-doped germanium and germanium clusters by the density-functional theory. *J. Chem. Phys.* **2005**, *123*, 244303.
- [12] Wang, J.; Han, J.-G. A Theoretical Study on Growth Patterns of Ni-Doped Germanium Clusters. *J. Phys. Chem. B* **2006**, *11*, 7820-7827.
- [13] Wang, J.; Han, J.-G. Geometries and electronic properties of the tungsten-doped germanium clusters: WGe_n (n = 1-17). *J. Phys. Chem. A* **2006**, *110*, 12670-12677.
- [14] Wang, J.; Han, J.-G. Geometries, stabilities, and vibrational properties of bimetallic Mo₂-doped Ge_n (n = 9-15) clusters: a density functional investigation. *J. Phys. Chem. A* **2008**, *112*, 3224-3230.
- [15] Trivedi, R.; Dhaka, K.; Bandyopadhyay, D. Study of electronic properties, stabilities and magnetic quenching of molybdenum-doped germanium clusters: a density functional investigation, *RSC Adv.* **2014**, *4*, 64825-64834.
- [16] Jing, Q.; Tian, F.-Y.; Wang, Y.-X. No quenching of magnetic moment for the Ge_nCo (n=1–13) clusters: First-principles calculations. *J. Chem. Phys.* **2008**, *128*, 124319.
- [17] Deng, X.-J.; Kong, X. Y.; Xu X-L; Xu H-G; Zheng W-J, Structural and magnetic properties of CoGe_n⁻ (n=2–11) clusters: photoelectron spectroscopy and density functional calculations. *Chem. Phys. Chem.* **2014**, *15*, 3987-3993.
- [18] Kumar Singh, A.; Kumar, V.; Kawazoe Y. Thorium encapsulated caged clusters of germanium: Th@Ge_n, n =16, 18, and 20. *J. Phys. Chem. B* **2005**, *109*, 15187-15189.

- [19] Zdetsis, A. D. Silicon-bismuth and germanium-bismuth clusters of high stability. *J. Phys. Chem. A* **2009**, *113*, 12079-12087.
- [20] Jaiswal, S.; Kumar, V. Growth behavior and electronic structure of neutral and anion $ZrGe_n$ ($n = 1-21$) clusters. *Comp. Theo. Chem.* **2016**, *1075*, 87-97.
- [21] Jin, Y.; Tian, Y.; Kuang, X.; Lu, C.; Cabellos, J.L.; Mondal, S.; Merino, G. Structural and electronic properties of ruthenium-doped germanium clusters. *J. Phys. Chem. C*, **2016**, *120*, 8399-8404.
- [22] Siouani, C.; Mahtout, S.; Safer, S.; Rabilloud, F. Structure, Stability, and electronic and magnetic properties of VGe_n ($n = 1-19$) clusters. *J. Phys. Chem. A* **2017**, *121*, 3540-3554.
- [23] Atobe, J.; Koyasu, K.; Furuse, S.; Nakajima, A. Anion photoelectron spectroscopy of germanium and tin clusters containing a transition-or lanthanide-metal atom; MGe_n^- ($n=8-20$) and MSn_n^- ($n=15-17$) ($M = Sc-V, Y-Nb, \text{ and } Lu-Ta$). *Phys. Chem. Chem. Phys.* **2012**, *14*, 9403-9410.
- [24] Li, X.; Su, K.; Yang, X.; Song, L.; Yang, L. Size-selective effects in the geometry and electronic property of bimetallic Au-Ge nanoclusters. *Comp. Theo. Chem.* **2013**, *1010*, 32-37.
- [25] Lu, S.-J.; Hu, L.-R.; Xu, X.-L.; Xu, H.-G.; Chen, H.; Zheng W.-J. Transition from exohedral to endohedral structures of $AuGe_n$ ($n = 2-12$) clusters: photoelectron spectroscopy and *ab initio* calculations. *Phys. Chem. Chem. Phys.* **2016**, *18*, 20321.
- [26] Bandyopadhyay, D.; Architectures, electronic structures, and stabilities of Cu-doped Ge_n clusters: density functional modeling. *J Mol Model.* **2012**, *18*, 3887-902.
- [27] Tai, T. B.; Nguyen, M. T.; Enhanced stability by three-dimensional aromaticity of endohedrally doped clusters $X_{10}M^{0/+}$ with $X = Ge, Sn, Pb$ and $M = Cu, Ag, Au$. *J. Phys. Chem. A* **2011**, *115*, 9993-9999.
- [28] Tai, T. B.; Nguyen, H. M. T.; Nguyen, M. T. The group 14 cationic clusters by encapsulation of coinage metals $X_{10}M^+$, with $X = Ge, Sn, Pb$ and $M = Cu, Ag, Au$: Enhanced stability of 40 valence electron systems. *Chem. Phys. Lett.* **2011**, *502*, 187-193.
- [29] Qin, W.; Lu, W.-C.; Xia, L.-H.; Zhao, L.-Z.; Zang, Q.-J.; Wang, C. Z.; Ho, K. M. Structures and stability of metal-doped Ge_nM ($n = 9, 10$) clusters. *AIP Advances* **2015**, *5*, 067159.
- [30] Brack, M. The physics of simple metal clusters: self-consistent jellium model and semiclassical approaches. *Rev. Mod. Phys.* **1993**, *65*, 677.
- [31] Samanta, P. N.; Das, K. K. Electronic structure, bonding, and properties of Sn_mGe_n ($m + n \leq 5$) clusters: A DFT study. *Comp. Theo Chem* **2012**, *980*, 123-132.
- [32] Tang, C.; Liu, M.; Zhu, W.; Deng, K. Probing the geometric, optical, and magnetic properties of 3d transition-metal endohedral $Ge_{12}M$ ($M = Sc-Ni$) clusters. *Comp. Theo. Chem.* **2011**, *969* 56-60.
- [33] Goswami, S.; Saha, S.; Yadav, R. K. Structural, electronic and vibrational properties of Ge_xC_y ($x+y=2-5$) nanoclusters: A B3LYP-DFT study. *Physica E* **2015**, *74*, 175-192.
- [34] Perdew, J.P.; Burke, K.; Ernzerhof, M. Generalized Gradient Approximation Made Simple. *Phys. Rev. Lett.* **1996**, *77*, 3865-3868.
- [35] Troullier, N.; Martins, J. L. Efficient pseudopotentials for plane-wave calculations. *Phys. Rev. B* **1991**, *43*, 1993.
- [36] Kleinman L.; Bylander, D.M. Efficacious form for model pseudopotentials. *Phys. Rev. Lett.* **1982**, *48*, 1425.
- [37] Ordejón, P.; Artacho E.; Soler, J. M. Self-consistent order-N density-functional calculations for very large systems. *Phys. Rev. B (Rapid Comm.)* **1996**, *53*, 10441; Soler, J. M.; Artacho, .; Gale, J. D.; García, A.; Junquera, J.; Ordejón, P.; Sánchez-Portal, D. The SIESTA method for ab initio order-N materials simulation. *J. Phys.: Condens. Mat.* **2002**, *14*, 2745.
- [38] Frisch M.J. et al., *Gaussian09*, Revision D.01, Gaussian Inc., Wallingford CT, 2013.

- [39] Shi, S.; Liu, Y.; Zhang, C.; Deng, B.; Jiang, G. A computational investigation of aluminum-doped germanium clusters by density functional theory study. *Comp. Theo. Chem.* **2015**, *1054*, 8-15.
- [40] Deutsch, P.W.; Curtiss, L.A.; Blaudeau, J.P. Binding energies of germanium clusters Ge_n ($n = 2-5$), *Chem. Phys. Lett.* **1997**, *270*, 413-418.
- [41] Nagendran, S.; Sen, S.S.; Roesky, H.W.; Koley, D.; Grubmüller, H.; Pal A.; Herbst-Irmer R.R Ge(I) Ge(I)R compound ($R = PhC(NtBu)_2$) with a Ge-Ge single bond and a comparison with the gauche conformation of hydrazine. *Organometallics* **2008**, *27*, 5459–5463.
- [42] Gadiyak, G.V.; Morokov, Y.N.; Mukhachev, A.G.; Chernov, S.V. Electron density functional method for molecular system calculations. *J. Struct. Chem.* **1982**, *22*, 670-674.
- [43] Beutel, V.; Kramer, H. G.; Bhale, G.L.; Kuhn, M.; Weyers, L.; Demtroder, W. High resolution isotope selective laser spectroscopy of Ag_2 molecules. *J. Chem. Phys.* **1992**, *98*, 2699.
- [44] Simard, B.; Hackett, P. A. High resolution study of the (0, 0) and (1, 1) bands of the $A0_u^+ - X0_g^+$ system of Au_2 . *J. Mol. Spectros.* **1990**, *142*, 310–318.
- [45] Ram, R. S.; Jarman, C. N.; Bernath, P. F. Fourier transform emission spectroscopy of the copper dimer. *J. Mol. Spectrosc.* **1992**, *156*, 468-486.
- [46] Kingcade, J.E.; Nagarathna-Naik, H. M.; Shim, I.; Gingerich, K. A. Electronic structure and bonding of the molecule Ge_2 from all-electron ab initio calculations and equilibrium measurements. *J. Phys. Chem.* **1986**, *90*, 2830-2834.
- [47] Rabilloud, F. Structure and stability of coinage metal fluoride and chloride clusters (M_nF_n and M_nCl_n , $M = Cu, Ag, \text{ or } Au$; $n = 1-6$). *J. Comp. Chem.* **2012**, *33*, 2083–2091.
- [48] Li, X.-J.; Su, K.-H. Structure, stability and electronic property of the gold-doped germanium clusters: $AuGe_n$ ($n = 2-13$). *Theor. Chem. Acc.* **2009**, *124*, 345.
- [49] Goicoechea, J. M.; McGrady, J. E. On the structural landscape in endohedral silicon and germanium clusters, $M@Si_{12}$ and $M@Ge_{12}$. *Dalton Trans.* **2015**, *44*, 6755-6766.
- [50] Espinoza-Quintero G.; Duckworth, J. C. A.; Myers, W. K.; McGrady, J. E.; Goicoechea, J. M. Synthesis and characterization of $[Ru@Ge_{12}]^{3-}$: An endohedral 3-connected cluster. *J. Am. Chem. Soc.* **2014**, *136*, 1210-1213.
- [51] L’Hermite, J.M.; Rabilloud, F.; Marcou, L.; Labastie, P. Metastable fragmentation of silver bromide clusters. *Eur. Phys. J. D* **2001**, *14*, 323-330.
- [52] Neukermans, S.; Wang, X.; Veldeman, N.; Janssens, E.; Silverans, R. E.; Lievens, P. Mass spectrometric stability study of binary MS_n clusters ($S = Si, Ge, Sn, Pn$, and $M = Cr, Mn, Cu, Zn$). *Int. J. Mass Spectrometry* **2006**, *252*, 145-150.

Table 1. Symmetry group, Binding energy per atom E_b (eV/atom), HOMO-LUMO gap ΔE (eV), Vertical Ionization Potential (VIP) (eV), Vertical Electronic Affinity (VEA) (eV), and average bond length $a_{\text{Ge-Ge}}$ and $a_{\text{Ge-Ag}}$ for AgGe_n (n=1-19) clusters.

n	Sym	E_b (eV/atom)	ΔE (eV)	VIP (eV)	VEA (eV)	$a_{\text{Ge-Ge}}$ (Å)	$a_{\text{Ge-Ag}}$ (Å)
1	a- C_{2v}	0.813	0.554	6.897	1.169	-	2.591
2	a- D_{2h}	0.988	0.404	6.916	1.653	-	2.567
	b- C_{2v}	1.721	0.206	6.945	1.571	2.339	2.696
3	a- C_{2v}	2.032	0.885	7.280	1.913	2.446	2.620
	b- C_s	1.999	0.618	6.835	1.372	2.667	2.828
4	a- C_s	2.324	1.127	6.602	1.651	2.623	2.860
	b- C_{2v}	2.306	0.873	6.787	1.711	2.674	2.907
	c- C_{2v}	2.113	0.486	6.798	1.991	2.421	2.823
5	a- C_1	2.376	0.758	6.595	1.940	2.570	2.811
	b- C_s	2.572	1.060	7.216	2.038	2.702	2.783
	c- C_{2v}	2.256	0.465	6.963	2.492	2.542	2.784
6	a- C_s	2.557	0.326	6.905	2.566	2.666	2.855
	b- C_s	2.662	1.156	6.783	2.131	2.764	2.849
	c- C_{2v}	2.650	1.017	6.747	1.982	2.765	2.827
	d- C_1	2.603	0.936	6.418	1.732	2.673	2.783
7	a- C_s	2.712	0.688	6.346	1.969	2.756	2.758
	b- C_1	2.695	0.708	6.337	1.984	2.772	2.809
	c- C_{2v}	2.656	0.476	6.686	2.278	2.737	2.864
8	a- C_s	2.778	0.665	6.610	2.378	2.750	2.789
	b- C_1	2.743	0.859	6.419	2.116	2.758	2.788
	c- C_1	2.762	0.582	6.612	2.328	2.787	2.780
	d- C_s	2.755	0.782	6.843	2.447	2.740	2.914
9	a- C_s	2.784	0.755	6.512	2.436	2.767	2.724
	b- C_1	2.797	0.667	6.267	2.223	2.774	2.789
	c- C_1	2.792	0.657	6.296	2.142	2.760	2.752
	d- C_1	2.794	0.758	6.403	2.204	2.711	2.802
	e- C_1	2.808	0.754	6.132	2.222	2.742	2.765
	f- C_1	2.804	0.884	6.442	2.416	2.756	2.851
	g- C_1	2.806	0.921	6.254	2.107	2.766	2.813
10	a- C_1	2.849	1.015	6.315	2.278	2.762	2.829
	b- C_s	2.898	0.611	6.667	2.719	2.800	2.768
	c- C_s	2.818	0.422	6.888	2.916	2.804	2.863
	d- C_s	2.835	0.762	6.660	2.725	2.752	2.951
11	a- C_1	2.828	0.380	6.652	2.836	2.778	2.834
	b- C_s	2.848	0.547	5.918	2.175	2.707	2.598
	c- C_1	2.869	0.380	6.637	2.802	2.806	2.803
	d- C_1	2.847	0.729	6.271	2.550	2.765	2.922
	e- C_{2v}	2.893	0.568	6.663	2.623	2.779	2.764
12	a- D_{3d}	2.919	0.236	7.120	3.356	2.950	2.805
	b- C_s	2.870	0.555	6.525	2.800	2.795	2.761
	c- C_1	2.866	0.416	6.525	2.856	2.719	2.857
	d- C_s	2.879	0.342	6.463	2.794	2.826	2.837
	e- C_{2h}	2.910	0.126	6.383	2.892	2.653	2.878
	f- d_{2d}	2.926	0.744	6.390	2.699	2.661	2.879
	g- C_1	2.879	0.566	6.383	2.712	2.794	2.778
13	b- C_{2v}	2.890	0.765	6.084	2.462	2.789	2.742
	c- C_1	2.906	0.655	6.448	2.854	2.758	2.891
	d- C_1	2.903	0.495	6.508	2.996	2.780	2.866
	e- C_1	2.914	0.750	6.359	2.715	2.797	2.797
	f- C_1	2.879	0.566	6.383	2.712	2.794	2.778
	g- C_1	2.890	0.765	6.084	2.462	2.789	2.742
14	a- D_{4h}	2.963	0.171	6.495	3.029	2.736	2.949
	b- C_1	2.911	0.638	6.238	2.769	2.766	2.771
	c- C_1	2.917	0.627	6.331	2.880	2.746	2.907
	d- C_1	2.952	0.552	6.514	2.861	2.791	2.922
15	a- C_1	2.947	0.786	6.167	2.706	2.788	2.841
	b- C_1	2.932	0.586	6.245	2.905	2.771	2.885
	c- C_{2v}	3.019	0.732	6.662	3.024	2.762	2.886
	d- C_1	2.946	0.594	6.157	2.772	2.774	2.913
16	a- C_1	2.964	0.511	6.358	2.880	2.806	2.937
	b- C_1	2.919	0.476	6.278	2.918	2.770	2.847
	c- C_1	2.985	0.336	6.581	3.274	2.784	2.886
	d- C_s	2.915	0.405	6.045	2.841	2.813	2.823
	e- C_1	2.943	0.618	6.074	2.808	2.827	2.886
17	a- C_1	2.933	0.583	6.028	2.631	2.853	2.909
	b- C_1	2.966	0.601	6.116	2.818	2.819	3.009
	c- C_1	2.940	0.455	6.192	2.991	2.750	2.967
	d- C_1	2.942	0.589	5.839	2.508	2.755	2.912
18	a- C_1	2.991	0.708	6.076	2.817	2.783	2.876
	b- C_1	2.988	0.583	6.172	1.551	2.744	2.841
	c- C_1	2.978	0.698	6.059	2.791	2.766	2.935
	d- C_1	2.987	0.623	6.034	2.796	2.714	2.948
	e- C_1	2.981	0.615	6.082	2.784	2.787	2.682
19	a- C_1	3.017	0.437	6.304	3.086	2.802	2.953
	b- C_1	2.973	0.439	6.362	3.119	2.737	2.887
	c- C_1	3.001	0.600	6.199	3.038	2.756	2.946
	d- C_{3v}	2.990	0.644	6.223	2.906	2.743	2.942
	e- C_1	2.988	0.542	6.253	3.082	2.797	2.967
	f- C_{2v}	2.976	0.445	6.217	3.021	2.720	2.969

Table 2. Symmetry group, Binding energy per atom E_b (eV/atom), HOMO-LUMO gap ΔE (eV), Vertical Ionization Potential (VIP) (eV), Vertical Electronic Affinity (VEA) (eV), and average bond length $a_{\text{Ge-Ge}}$ and $a_{\text{Ge-Au}}$ for AuGe_n ($n=1-19$) clusters.

n	Sym	E_b (eV/atom)	ΔE (eV)	VIP (eV)	VEA (eV)	$a_{\text{Ge-Ge}}$ (Å)	$a_{\text{Ge-Au}}$ (Å)
1	a- C_{3v}	0.813	1.354	6.931	1.227	-	2.645
2	a- D_{3h}	0.997	0.469	6.924	1.660	-	2.619
	b- C_{2v}	1.697	0.177	6.913	1.608	2.347	2.762
3	a- C_{2v}	2.015	0.910	7.208	1.893	2.451	2.680
	b- C_s	1.985	0.627	6.806	1.385	2.672	2.892
	c- C_{2v}	1.981	0.388	6.441	1.400	2.434	2.849
4	a- C_s	2.300	0.849	6.902	1.853	2.665	2.848
	b- C_{2v}	2.093	0.468	6.781	1.983	2.426	2.882
	c- C_s	2.310	1.103	6.596	1.698	2.623	2.936
5	a- C_{2v}	2.550	1.127	7.167	2.017	2.698	2.736
	b- C_s	2.553	1.059	7.194	2.050	2.705	2.854
	c- C_{2v}	2.494	1.273	6.767	2.090	2.656	2.780
6	a- C_s	2.538	0.570	6.731	2.362	2.661	2.927
	b- C_s	2.655	1.144	6.677	1.976	2.703	2.846
	c- C_{2v}	2.627	0.951	6.678	1.953	2.769	2.904
7	a- C_1	2.464	0.643	6.559	2.521	2.525	2.833
	b- C_s	2.696	1.141	6.421	2.053	2.723	2.838
	c- C_1	2.681	0.949	6.492	2.091	2.739	2.813
	d- C_{2v}	2.648	0.479	6.670	2.276	2.737	2.927
8	a- C_s	2.764	0.654	6.585	2.372	2.752	2.854
	b- C_2	2.740	0.645	6.500	2.220	2.789	2.879
	c- C_1	2.709	0.526	6.989	2.679	2.758	2.915
	d- C_s	2.742	0.746	6.821	2.453	2.746	2.972
9	a- C_s	2.772	0.785	6.476	2.424	2.767	2.793
	b- C_1	2.785	0.616	6.201	2.200	2.755	2.853
	c- C_{2v}	2.765	0.902	6.238	2.216	2.791	3.070
	d- C_1	2.782	0.693	6.340	2.176	2.713	2.873
	e- C_1	2.797	0.793	6.149	2.257	2.743	2.833
	f- C_1	2.795	0.973	6.283	2.141	2.764	2.723
10	a- C_1	2.838	0.975	6.320	2.298	2.763	2.803
	b- C_s	2.794	0.484	6.816	2.871	2.822	2.915
	c- C_s	2.797	0.912	6.088	2.207	2.743	2.974
11	a- C_1	2.817	0.517	6.535	2.757	2.752	2.833
	b- C_s	2.838	0.507	5.899	2.168	2.708	2.662
	c- C_1	2.831	0.743	6.117	2.367	2.789	2.780
	d- C_1	2.834	0.722	6.256	2.541	2.767	2.887
	e- C_{2v}	2.882	0.535	6.687	2.659	2.781	2.832
12	a- C_2	2.875	0.586	6.718	2.999	2.824	2.937
	b- C_s	2.863	0.553	6.511	2.799	2.795	2.818
	c- C_1	2.858	0.450	6.516	2.856	2.717	2.822
	d- C_s	2.866	0.348	6.396	2.749	2.828	2.915
	e- C_s	2.885	0.374	6.422	2.746	2.715	2.904
	f- D_{2d}	2.912	0.733	6.401	2.726	2.680	2.901
13	a- C_{2v}	2.871	0.575	6.370	2.701	2.793	2.841
	b- C_s	2.865	0.617	5.854	2.374	2.804	2.875
	c- C_1	2.919	0.831	6.297	2.736	2.759	2.904
	d- C_1	2.889	0.444	6.487	2.997	2.778	2.942
	e- C_1	2.904	0.751	6.350	2.717	2.799	2.864
	f- C_1	2.870	0.503	6.543	2.922	2.744	2.941
14	a- C_1	2.904	0.646	6.229	2.769	2.767	2.848
	b- D_{4h}	2.934	0.165	6.423	2.972	2.755	2.972
	c- C_1	2.933	0.594	6.486	2.815	2.807	2.969
15	a- C_1	2.946	0.841	6.016	2.682	2.771	2.918
	b- C_s	2.930	0.758	6.366	2.889	2.811	2.886
	c- C_s	2.997	0.495	6.609	3.201	2.791	2.789
	d- C_1	2.923	0.715	6.234	2.752	2.749	2.872
16	a- C_1	2.967	0.660	6.140	2.728	2.786	2.995
	b- C_1	2.912	0.474	6.311	2.927	2.771	2.908
	c- C_1	2.925	0.630	6.125	2.868	2.803	2.945
17	a- C_1	2.925	0.589	6.033	2.628	2.839	2.927
	b- C_1	2.974	0.499	6.132	2.831	2.734	2.957
	c- C_1	2.933	0.446	6.208	3.004	2.753	2.995
	d- C_1	2.948	0.494	6.063	2.754	2.769	2.872
18	a- C_1	3.004	0.656	6.194	2.780	2.775	2.932
	b- C_1	2.981	0.465	6.328	3.054	2.728	2.996
	c- C_1	2.973	0.643	6.115	2.903	2.780	2.965
	d- C_1	2.974	0.579	6.013	2.774	2.708	2.988
19	a- C_1	3.006	0.425	6.305	3.086	2.805	2.979
	b- C_1	2.999	0.600	6.029	2.906	2.770	2.977
	c- C_1	2.972	0.551	6.273	3.055	2.768	2.973
	d- C_{2v}	2.967	0.438	6.203	3.008	2.727	2.991

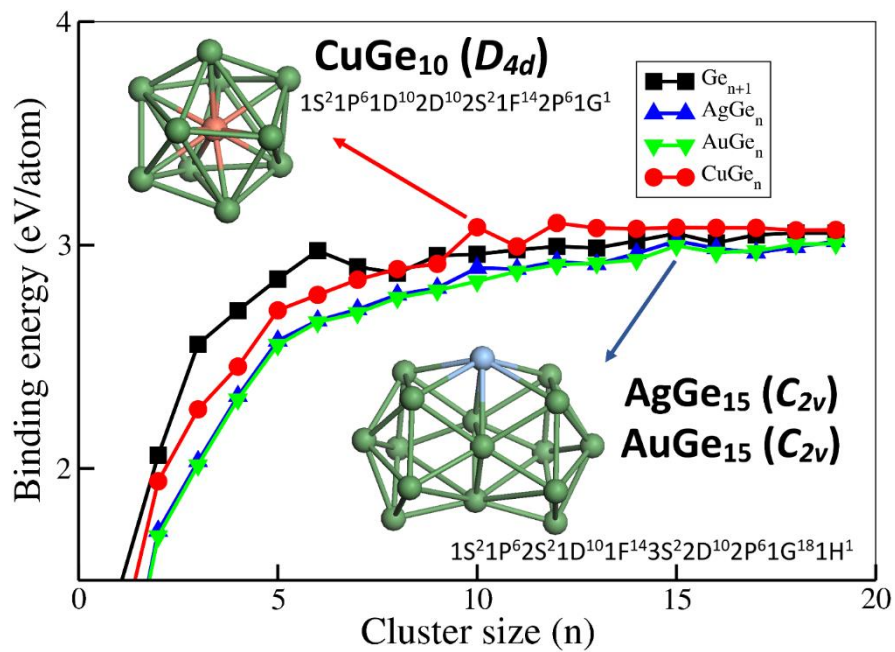
Table 3. Symmetry group, Binding energy per atom E_b (eV/atom), HOMO-LUMO gap ΔE (eV), Vertical Ionization Potential (VIP) (eV), Vertical Electronic Affinity (VEA) (eV), and average bond length $a_{\text{Ge-Ge}}$ and $a_{\text{Ge-Cu}}$ for CuGe_n ($n=1-19$) clusters.

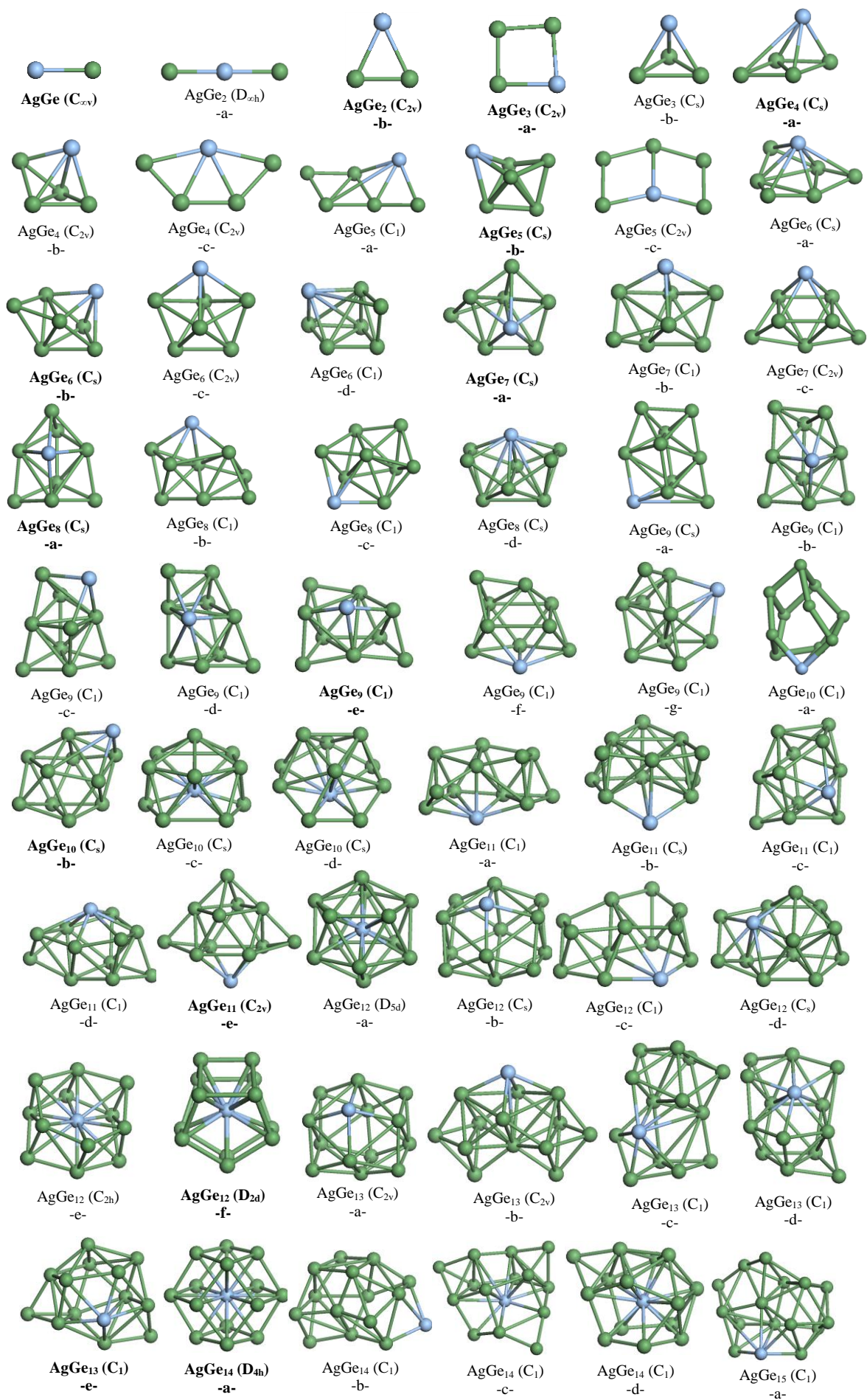
n	Sym	E_b (eV/atom)	ΔE (eV)	VIP (eV)	VEA (eV)	$a_{\text{Ge-Ge}}$ (Å)	$a_{\text{Ge-Cu}}$ (Å)
1	a- C_{xy}	1.185	0.991	6.992	1.039	-	2.333
2	a- D _{3h}	1.398	0.647	7.103	1.455	-	2.345
	b- C_{2v}	1.943	0.176	7.092	1.606	2.375	2.430
3	a- C_{2v}	2.265	0.825	7.501	1.954	2.464	2.366
	b- C _s	2.154	0.581	6.978	1.472	2.706	2.551
4	a- C_s	2.456	0.681	7.192	1.999	2.680	2.520
	b- C ₁	2.433	0.983	6.674	1.778	2.610	2.431
	c- C _{3v}	2.255	0.716	7.229	2.217	2.572	2.485
5	a- C _{2v}	2.701	1.205	7.271	2.100	2.703	2.700
	b- C_s	2.708	1.048	7.314	2.146	2.717	2.491
	c- C _s	2.535	0.301	6.970	2.416	2.638	2.608
6	a- C _{3v}	2.690	0.587	7.165	2.681	2.722	2.684
	b- C_{2v}	2.777	1.028	7.071	2.193	2.781	2.537
	c- C _s	2.701	0.420	7.195	2.658	2.532	2.601
	d- C ₁	2.726	0.574	6.492	1.799	2.754	2.581
7	a- C _s	2.826	0.316	6.342	1.982	2.722	2.482
	b- C_s	2.845	0.878	6.669	2.204	2.767	2.644
	c- C _s	2.805	0.302	6.985	2.601	2.783	2.598
	d- C _{2v}	2.757	0.554	6.742	2.304	2.746	2.591
8	a- C_s	2.893	0.744	6.729	2.475	2.754	2.527
	b- C ₁	2.857	0.881	6.590	2.256	2.766	2.506
	c- C _s	2.868	0.766	6.785	2.485	2.716	2.615
	d- C _s	2.883	0.847	6.939	2.525	2.741	2.640
9	a- C _s	2.888	0.600	6.695	2.578	2.822	2.485
	b- C ₁	2.900	0.726	6.439	2.337	2.777	2.525
	c- C _s	2.851	0.738	6.746	2.490	2.789	2.503
	d- C ₁	2.909	0.662	6.392	2.270	2.773	2.517
	e- C₁	2.916	0.667	6.867	2.666	2.774	2.611
10	a- C ₁	2.902	0.654	6.729	2.691	2.723	2.539
	b- C ₁	2.950	0.709	6.603	2.622	2.784	2.593
	c- D_{4d}	3.080	1.324	6.653	2.621	2.786	2.559
	d- C ₁	2.941	0.692	6.435	2.549	2.785	2.619
11	a- C₁	2.994	0.633	6.474	2.723	2.775	2.617
	b- C ₁	2.978	0.684	6.435	2.603	2.760	2.597
	c- C ₁	2.991	0.663	6.508	2.641	2.782	2.622
	d- C _{2v}	2.982	0.602	6.699	2.656	2.782	2.513
12	a- D_{5d}	3.099	0.304	7.046	3.228	2.877	2.735
	b- C _s	2.947	0.592	6.570	2.829	2.797	2.538
	c- C _s	3.008	0.550	6.601	2.832	2.835	2.619
	d- C _s	3.043	0.279	6.557	2.839	2.668	2.823
	e- C ₁	3.044	0.433	6.455	2.745	2.668	2.749
13	a- C ₁	3.045	0.525	6.589	2.938	2.738	2.707
	b- C_s	3.076	0.510	6.119	2.533	2.876	2.755
	c- C ₁	3.001	0.746	6.541	2.774	2.752	2.742
	d- C ₁	3.056	0.745	6.283	2.664	2.778	2.738
14	a- D_{4h}	3.073	0.189	6.612	3.091	2.697	2.900
	b- C ₁	3.065	0.596	6.488	2.923	2.803	2.836
	c- C ₁	3.028	0.380	6.155	2.684	2.723	2.780
	d- C ₁	3.068	0.617	6.391	2.784	2.805	2.605
15	a- C ₁	3.005	0.649	6.389	2.927	2.816	2.588
	b- C₁	3.079	0.664	6.345	2.871	2.813	2.834
	c- C _s	3.050	0.618	6.485	2.979	2.786	2.589
	d- C ₁	3.015	0.530	6.168	2.716	2.803	2.775
16	a- C₁	3.077	0.868	6.089	2.541	2.785	2.815
	b- C ₁	3.007	0.647	6.208	2.848	2.800	2.651
	c- C ₁	3.045	0.262	6.623	3.196	2.775	2.558
	d- C _s	2.995	0.555	7.955	2.882	2.808	2.562
17	a- C _s	2.997	0.512	5.977	2.629	2.857	2.558
	b- C ₁	3.066	0.600	6.157	2.748	2.838	2.760
	c- C ₁	3.027	0.738	6.131	2.746	2.794	2.778
	d- C₁	3.077	0.506	5.979	2.730	2.797	2.636
	e- C ₁	3.011	0.680	5.952	2.620	2.757	2.626
18	a- C_s	3.066	0.350	6.200	3.045	2.793	2.642
	b- C ₁	3.018	0.438	5.983	2.713	2.722	2.862
	c- C ₁	3.059	0.380	6.236	2.957	2.773	2.769
	d- C _s	3.051	0.427	6.272	2.992	2.774	2.750
19	a- C₁	3.068	0.353	6.250	3.032	2.761	2.826
	b- C ₁	3.049	0.388	6.449	3.139	2.799	2.585
	c- C ₁	3.054	0.611	6.040	2.786	2.822	2.537
	d- C _{2v}	3.047	0.262	6.224	3.096	2.741	2.765

Table 4. Electron shell configuration in endohedral cage-like structures MGe_n ($M = Cu, Ag, Au$; $n = 10, 12, 14$) and hollow cages of $AgGe_{15}$ and $AuGe_{15}$.

Clusters: electronic occupations in shell model
CuGe₁₀ (<i>D_{4d}</i>): $1S^2 1P^6 1D^{10} 2D^{10} 2S^2 1F^{14} 2P^6 1G^1$
CuGe₁₂ (<i>D_{5d}</i>): $1S^2 1P^6 1D^{10} 2D^{10} 2S^2 1F^{14} 2P^6 1G^9$
AgGe₁₂ (<i>D_{5d}, D_{2d}</i>): $1S^2 1P^6 1D^{10} 2D^{10} 2S^2 1F^{14} 2P^6 1G^9$
AuGe₁₂ (<i>D_{2d}</i>): $1S^2 1P^6 1D^{10} 2D^{10} 2S^2 1F^{14} 2P^6 1G^9$
AuGe₁₂ (<i>C_s</i>): $1S^2 1P^6 1D^{10} 2S^2 1F^{14} 2D^8 2P^6 1G^{11}$
CuGe₁₄ (<i>D_{4h}</i>): $1S^2 1P^6 1D^{10} 2S^2 1F^{14} 2D^{10} 3S^2 2P^6 1G^{15}$
AgGe₁₄ (<i>D_{4h}</i>): $1S^2 1P^6 1D^{10} 2S^2 1F^{14} 2D^{10} 3S^2 2P^6 1G^{15}$
AuGe₁₄ (<i>D_{4h}</i>): $1S^2 1P^6 1D^{10} 1F^{14} 2D^{10} 2S^2 3S^2 2P^6 1G^{15}$
AgGe₁₅ (<i>C_{2v}</i>): $1S^2 1P^6 2S^2 1D^{10} 1F^{14} 3S^2 2D^{10} 2P^6 1G^{18} 1H^1$
AuGe₁₅ (<i>C_s</i>): $1S^2 1P^6 2S^2 1D^{10} 1F^{14} 3S^2 2D^{10} 2P^6 1G^{18} 1H^1$

TOC





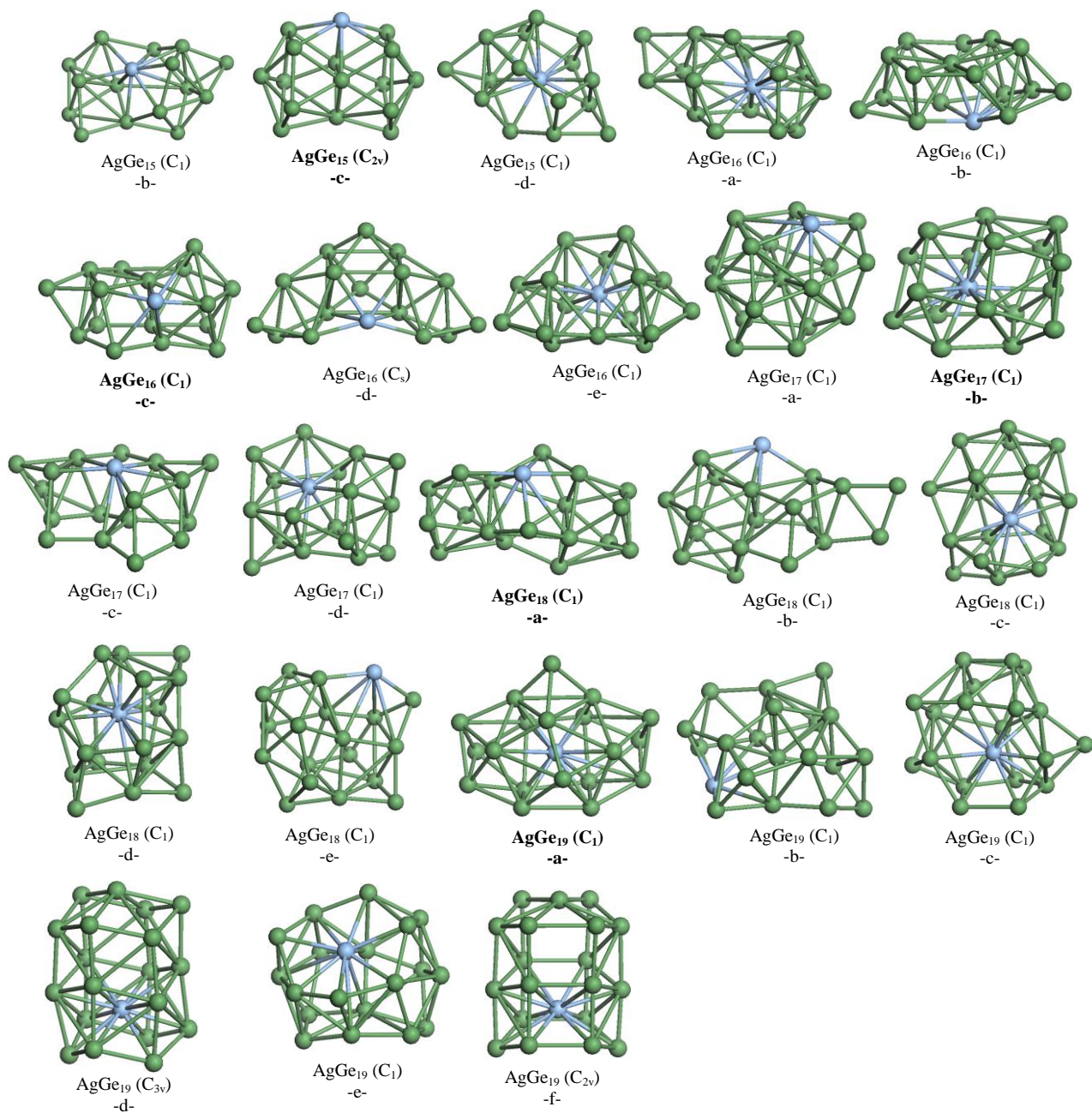
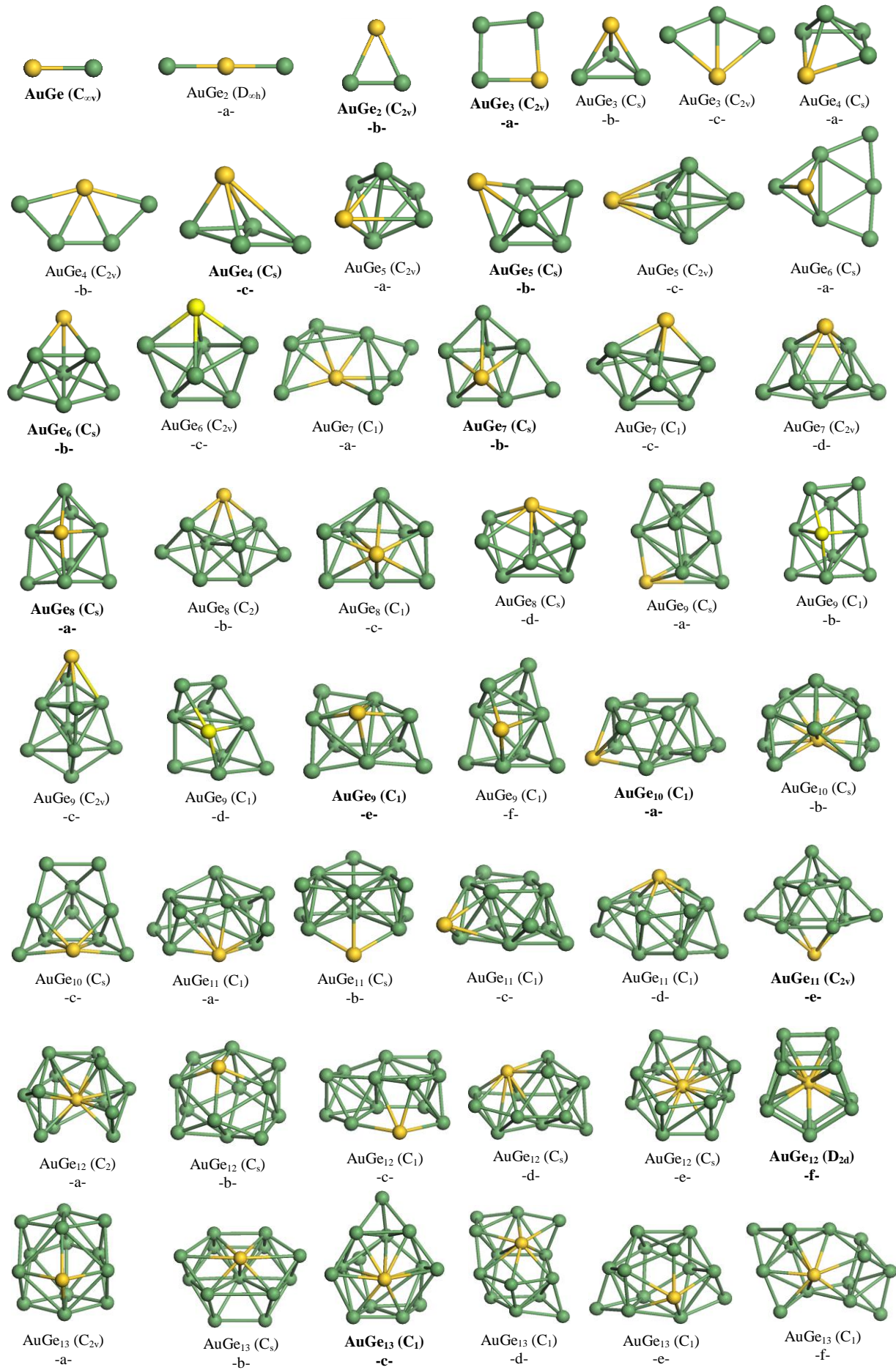


Figure 1. Ground-state structures and their corresponding isomers for AgGe_n ($n=1-19$) clusters. For each size, the lowest-energy isomer is indicated in bold characters.



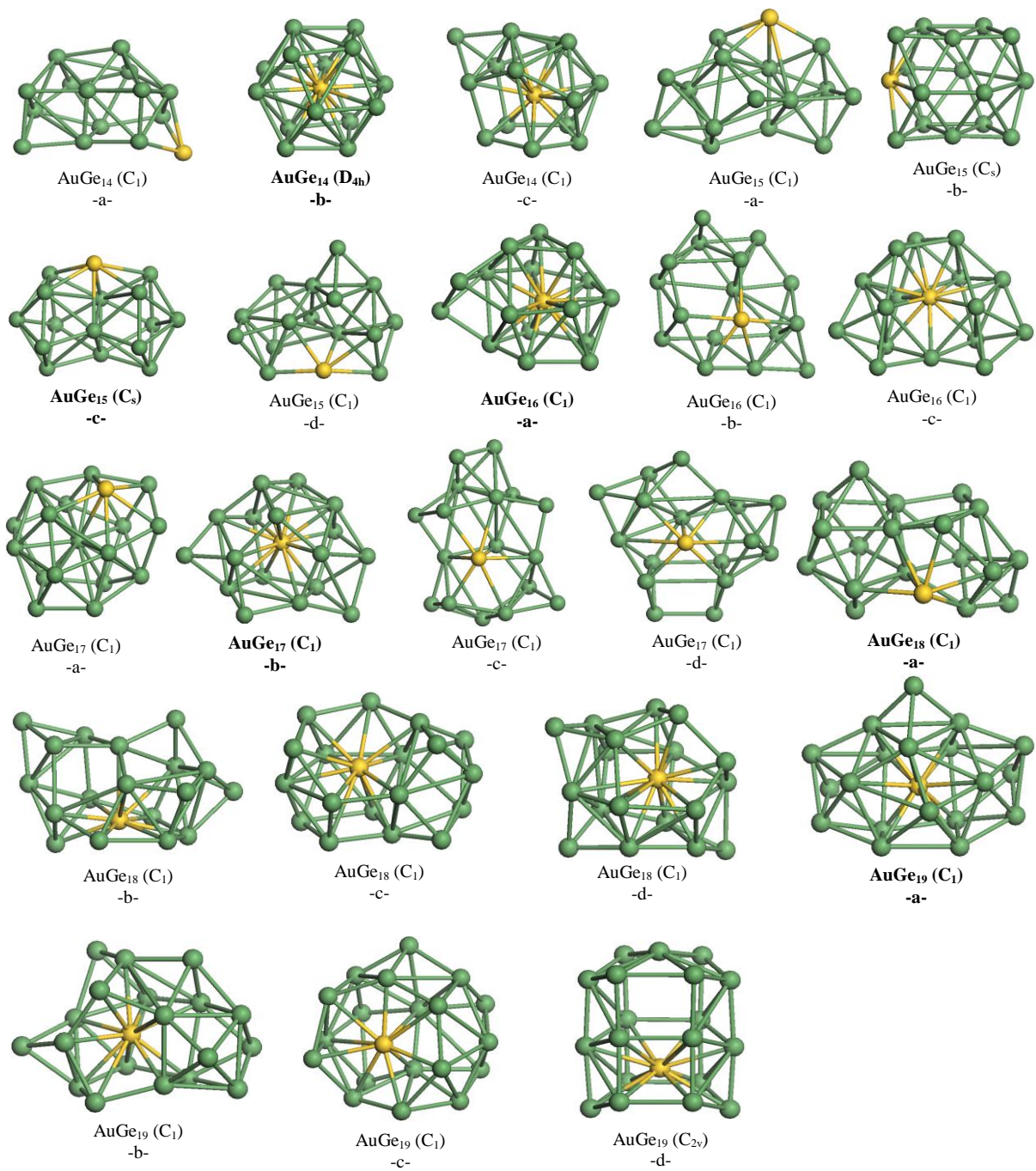
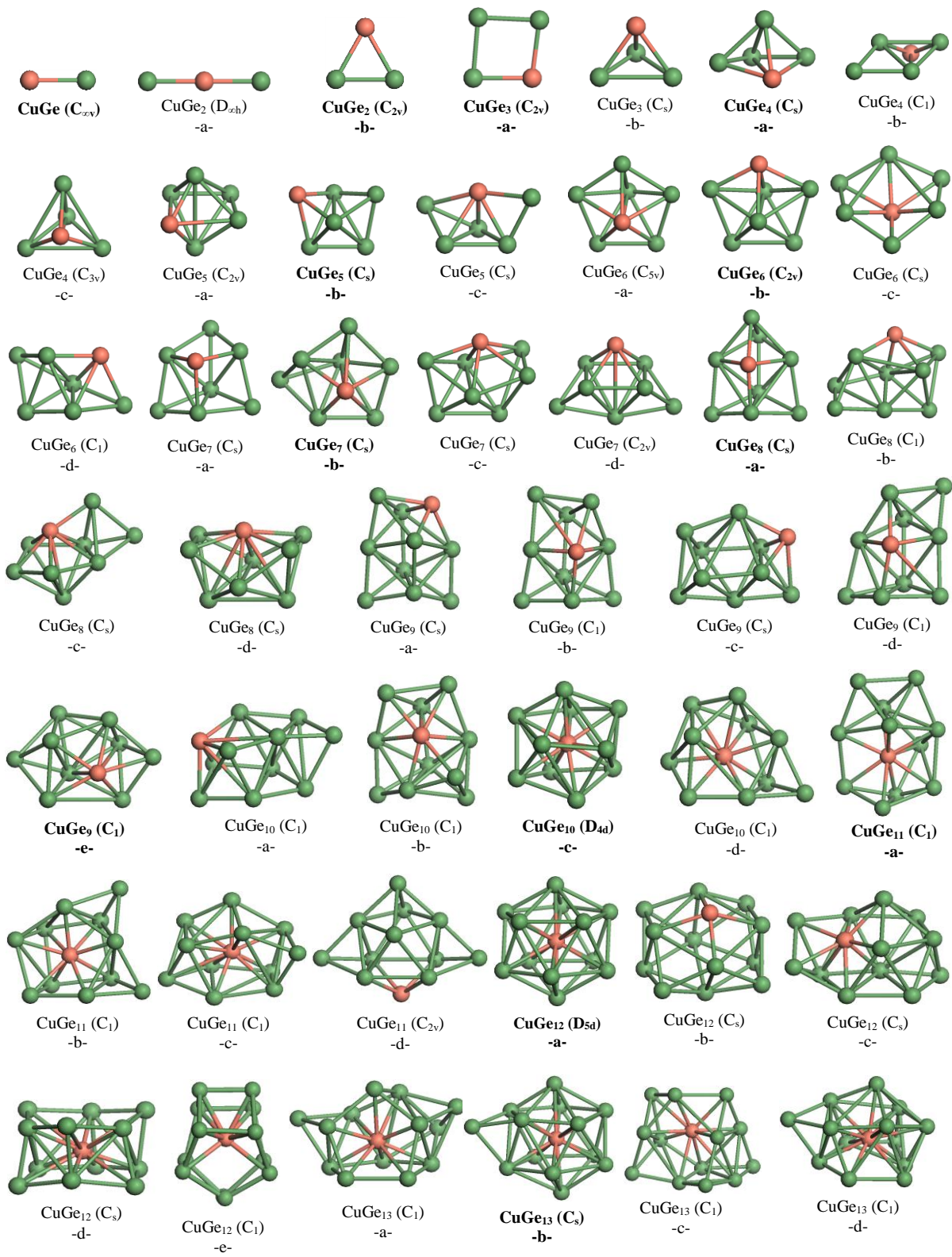


Figure 2. Ground state structures and their corresponding isomers for AuGe_n (n=1-19) clusters. For each size, the lowest-energy isomer is indicated in bold characters.



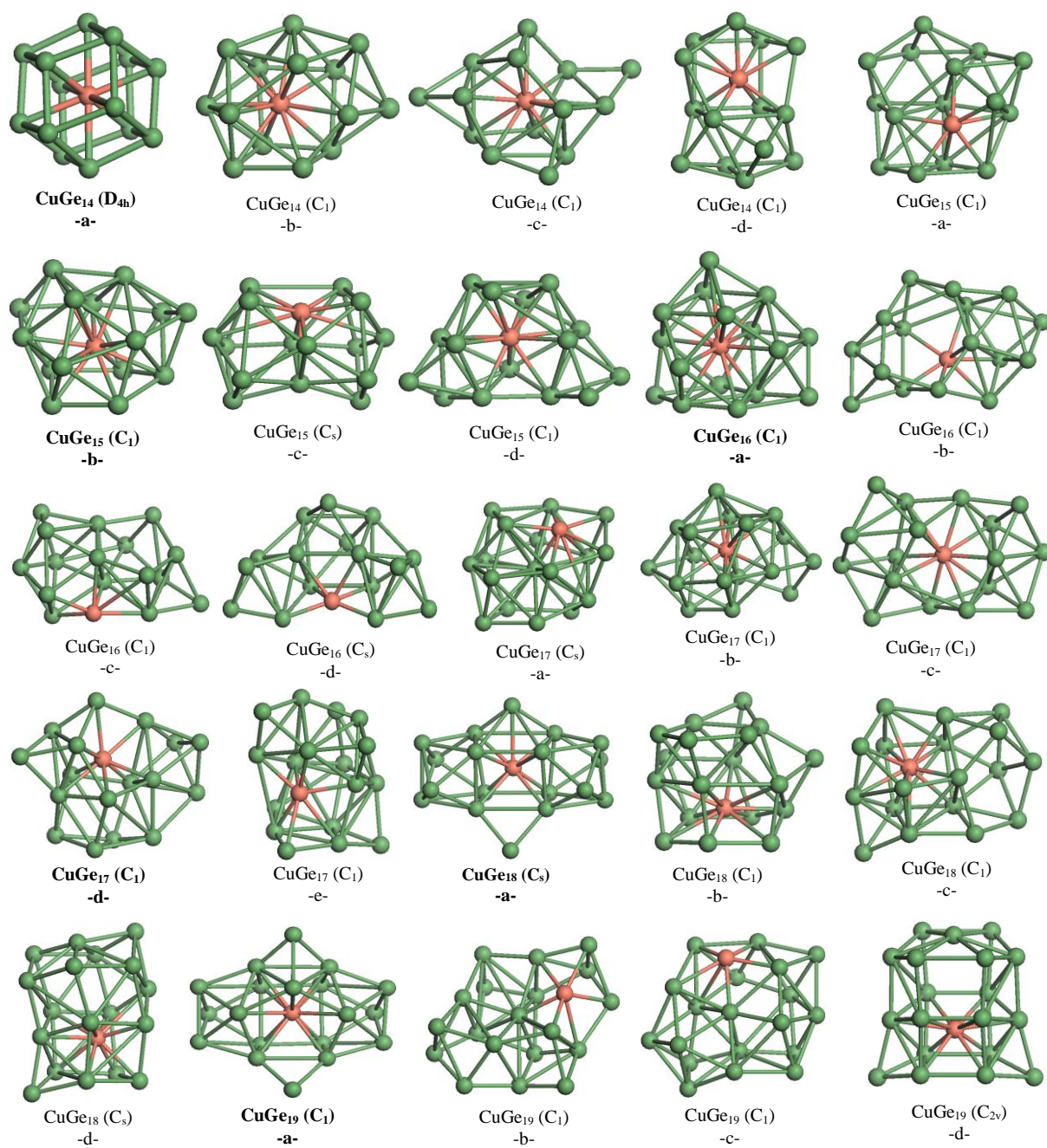


Figure 3. Ground state structures and their corresponding isomers for CuGe_n (n=1-19) clusters. For each size, the lowest-energy isomer is indicated in bold characters.

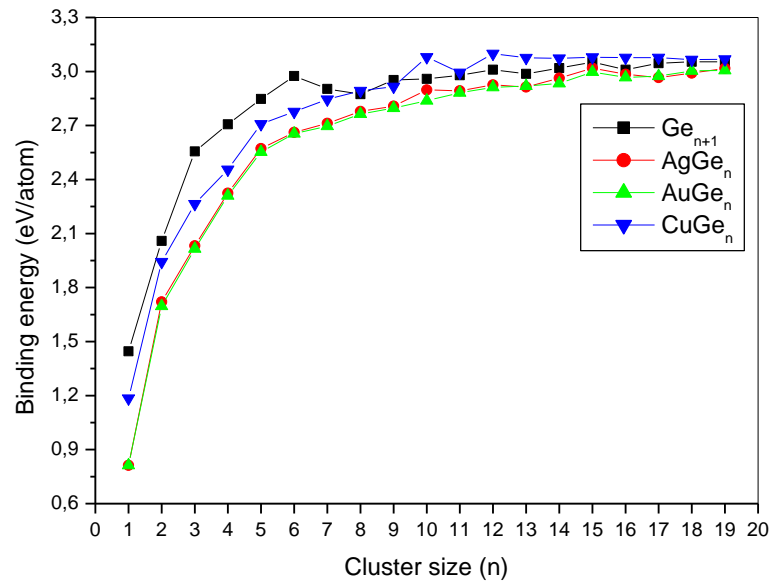


Figure 4. Size dependence of the binding energy per atoms for the ground state structures of MGe_n ($\text{M}=\text{Cu}, \text{Ag}, \text{Au}$) clusters.

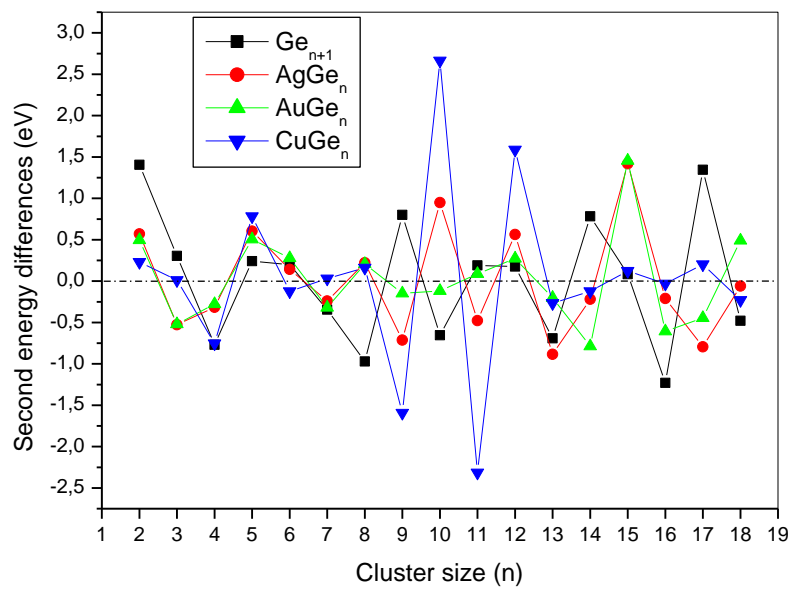


Figure 5. Second energy differences ($\Delta_2 E$) for the ground state structures of MGe_n (M =Cu, Ag, Au) clusters.

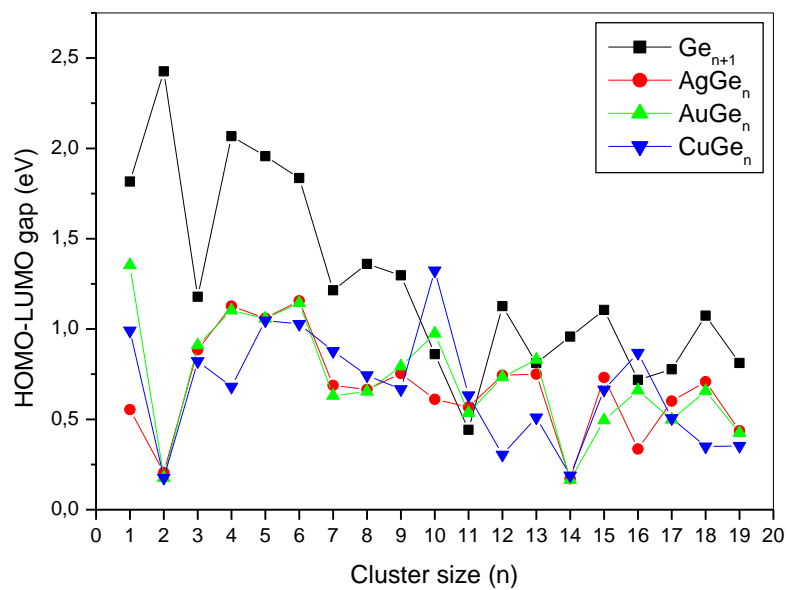


Figure 6. Size dependence of the HOMO-LUMO gap for the ground state structures of MGe_n ($M=Cu, Ag, Au$) clusters.

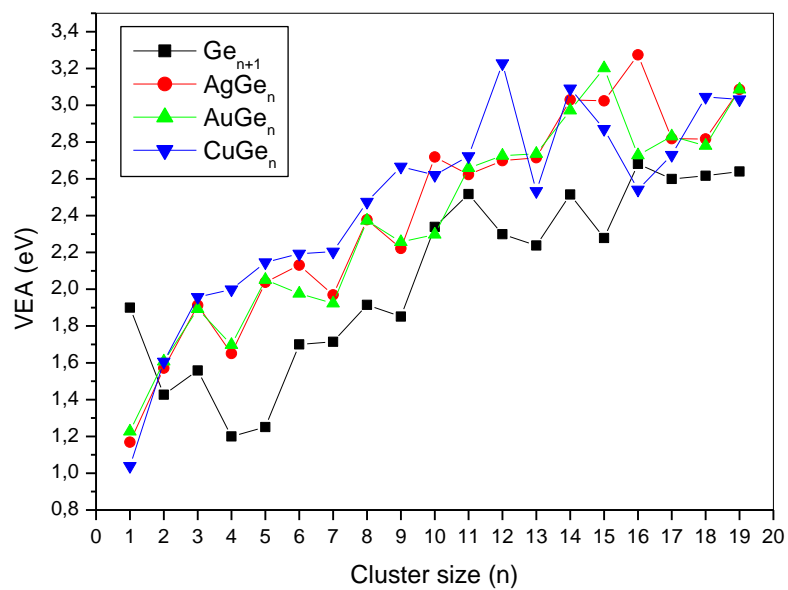


Figure 7. Size dependence of the vertical electron affinity for the ground state structures of MGe_n ($M=Cu, Ag, Au$) clusters.

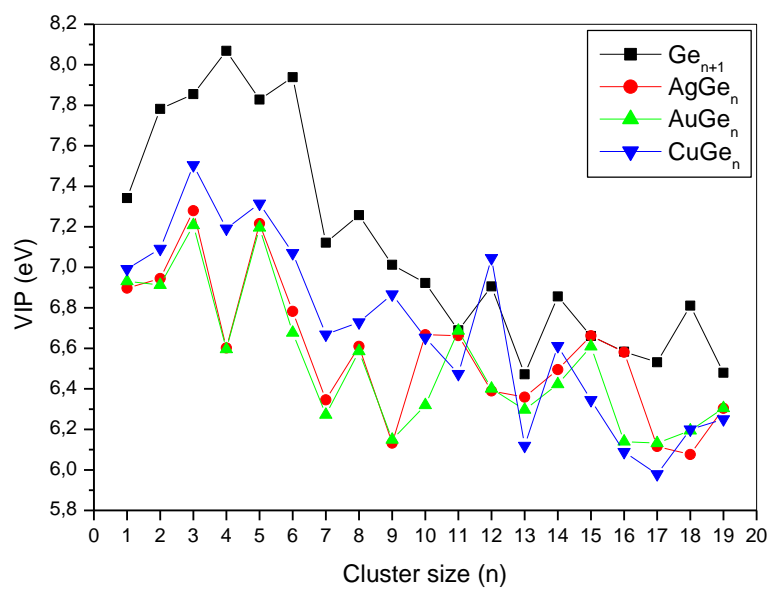


Figure 8. Size dependence of the vertical ionization potential for the ground state structures of MGe_n ($M=Cu, Ag, Au$) clusters.

Figure 9. Density of states for the most stable isomer of $\text{CuGe}_{10,12,14}$ together with some representative Kohn-Sham molecular orbitals. More molecular orbitals are given in Supporting Information.

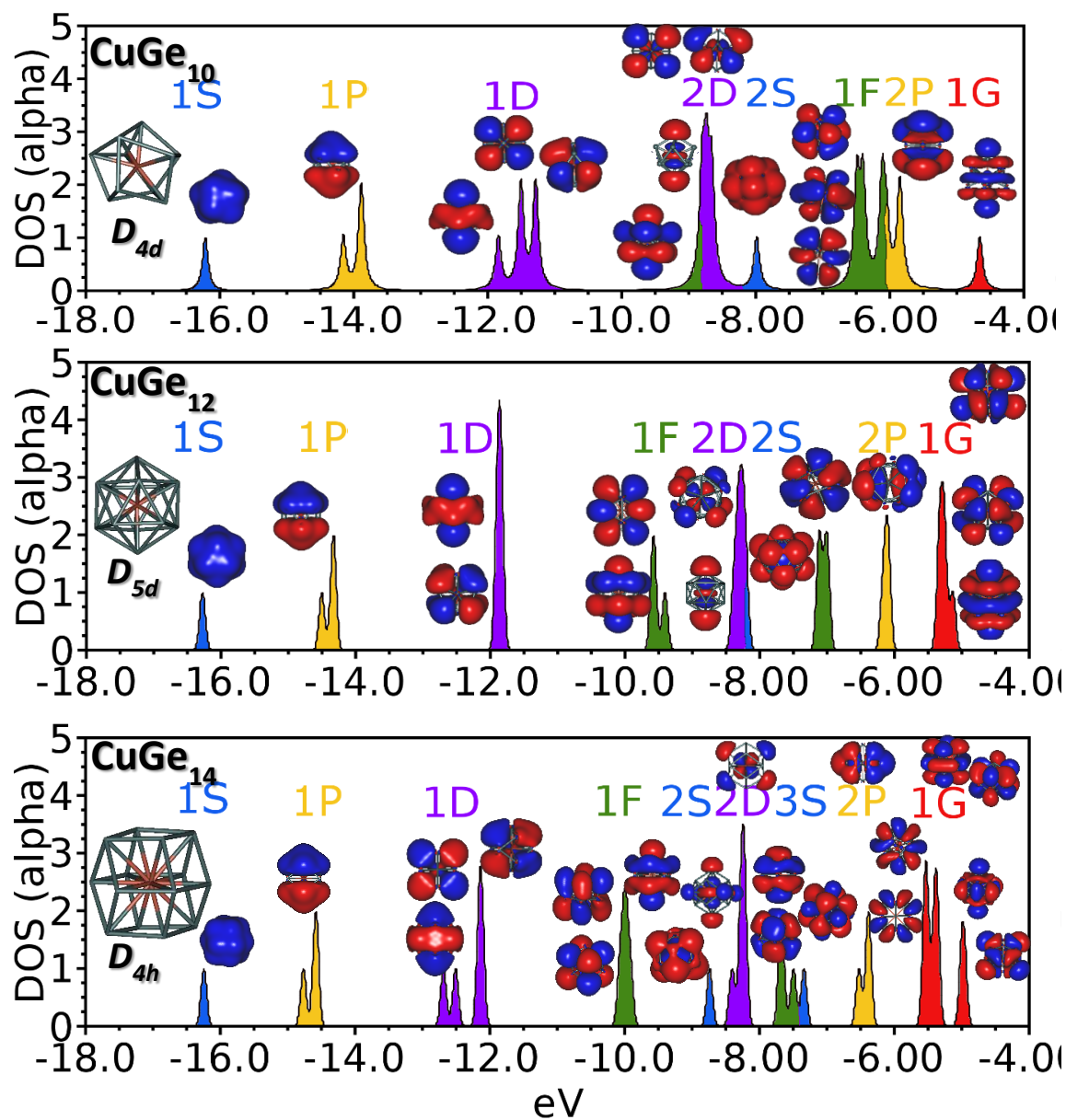


Figure 10. Density of states of the lowest-energy isomer of cage-like MGe_n ($M = Ag, Au$; $n=12, 14, 15$), i.e. an endohedral structure for $n=12$ and 14 , and a hollow cage for $n=15$. Kohn-Sham molecular orbitals are given in Supporting Information.

